Title Page

Dynamic changes in high and low mammographic density human breast tissues maintained in murine tissue engineering chambers during various murine peripartum states and over time

[1]G. L. Chew, [1]D. Huang, [1]C. W. Huo, [2]T. Blick, [3]P. Hill, [4]J. Cawson, [4]H. Frazer, [5]M. D. Southey, [5]J. L. Hopper, [6]M. A. Henderson, [3,7]I. Haviv, [1,2]E. W. Thompson

[1]University of Melbourne Department of Surgery, St. Vincent's Hospital, [2]St. Vincent's Institute, [3]Department of Pathology, University of Melbourne, [4]St Vincent's BreastScreen, St Vincent's Hospital Campus, University of Melbourne, [5]School of Population Health, University of Melbourne, [6]Peter MacCallum Cancer Center, [7] Department of Medicine, Bar Ilan University, Zfat, Israel.

Corresponding author: GL Chew; e-mail: grace.chew@svhm.org.au; telephone: +613 9288 2211; fax: +613 9288 4737

Abstract

Introduction: Mammographic density (MD) is a strong heritable risk factor for breast cancer, and may decrease with increasing parity. However, the biomolecular basis for MD-associated breast cancer remains unclear, and systemic hormonal effects on MD-associated risk is poorly understood. This study assessed the effect of murine peripartum states on high and low MD tissue maintained in a xenograft model of human MD.

Methods: High and low MD human breast tissues were precisely sampled under radiographic guidance from prophylactic mastectomy specimens of women. The high and low MD tissues were maintained in separate vascularised biochambers in nulliparous or pregnant SCID mice for four weeks, or mice undergoing postpartum involution or lactation for three additional weeks. High and low MD biochamber material was harvested for histologic and radiographic comparisons during various murine peripartum states. High and low MD biochamber tissues in nulliparous mice were harvested at different timepoints for histologic and radiographic comparisons.

Results: High MD biochamber tissues had decreased stromal ($p=0.0027$), increased adipose ($p=0.0003$) and a trend to increased glandular tissue areas ($p=0.076$) after murine postpartum involution. Stromal areas decreased ($p=0.042$), while glandular ($p=0.001$) and adipose areas ($p=0.009$) increased in high MD biochamber tissues during lactation. A difference in radiographic density was observed in high ($p=0.0021$) or low MD biochamber tissues ($p=0.004$) between nulliparous, pregnant and involution groups. No differences in tissue composition were observed in high or low MD biochamber tissues maintained for different durations, although radiographic density increased over time.

Conclusion: High MD biochamber tissues had decreased stromal, increased glandular and adipose tissue areas after postpartum involution or lactation. Alterations in radiographic density occurred in biochamber tissues between different peripartum states and over time. These findings demonstrate the dynamic nature of the human MD xenograft model, providing a platform for studying the biomolecular basis of MD-associated cancer risk.

Keywords: Mammographic density, xenograft, bioengineering chambers, stroma, adipose tissue, postpartum involution, lactation.

Introduction

Mammographic density (MD) is the area of radiologically white or bright tissue seen on a mammogram [1]. High MD adjusted for age and BMI is one of the strongest risk factors for breast cancer (BC), and carries a significant attributable risk for BC in the community [2-7]. Studies have previously demonstrated that BC risk is reduced in the longer-term after each live birth [8,9]. Parous women who have experienced a reduced number of ovulatory menstrual cycles had decreased BC risk [10-12]. Meanwhile, a negative association has been observed between parity and MD [13]. Other hormonal interventions, such as hormone replacement therapy (HRT) and Tamoxifen, alter MD as well as BC risk [14-18]. Only the women who had ≥10% decrease in MD with Tamoxifen in the IBIS-1 prevention trial benefited with BC risk reduction [18].

Previously we developed a xenograft model for the propagation of high and low MD regions of human breast tissue within *in vivo* paired biochambers placed on the epigastric pedicle of SCID mice [19,20]. Immunohistochemical analyses confirmed that human mammary glandular and stromal structures were maintained in the xenograft model [19]. The high and low MD histologic and radiographic phenotypes of biochamber tissues were also preserved in this model, consistent with the original human breast tissue samples [19,20].

It is likely that MD may be altered by changes in the systemic hormonal milieu [21]. To examine such effects upon MD, high and low MD regions from within individual human breast samples were maintained in murine biochambers and harvested after postpartum mammary involution, or lactation for three weeks, post-parturition or from nulliparous mice. Alterations to histologic and radiographic phenotypes in MD tissue would demonstrate that the model is dynamic, and that human breast tissue of varying MD responds to murine systemic hormonal changes or duration of maintenance in the biochamber environment.

Method

Accrual of high and low MD regions within the same breast

With approval from Peter MacCallum Human Research Ethics Committee (#08/21) and St. Vincent's Hospital Animal Ethics Committee (049/09), ten high-risk women undergoing prophylactic mastectomy at St Vincent's Hospital Melbourne were consented through the Victorian Cancer Biobank, Australia (VCB 10010). The mammograms of each participant were examined by a breast radiologist and their BIRADS category noted. Radiographic-guided sampling of high and low MD regions from within the same fresh breast specimen was performed by stereotactic biopsy (SenoRx 10G, Bard, Arizona, USA) or slice method, as previously described [19,20].

The high and low MD tissues were kept viable and sterile on ice, then separately partitioned for murine biochamber propagation, histologic (formalin-fixed, paraffin-embedded and OCT) and radiographic analyses, as well as future analysis (snap frozen in liquid nitrogen).

Maintenance in murine biochambers during pregnancy, postpartum involution, or lactation, and in nulliparous mice

High and low MD samples were minced, mixed 2:1 with Matrigel (BD Biosciences, Bedford, MA), supplemented with FGF-2 (1 μg/ml, Sigma-Aldrich, Sydney, Australia), and then separately transferred into silicone biochambers implanted in the groin based on the right and left epigastric pedicles respectively of multiple six week old female SCID mice (n = 12), as previously described [19,22-24].

The female mice were allowed to mate for three days, then the male mice removed from the cage. The females were examined for pregnancy after 3 weeks, and separated into nulliparous, pregnant, postpartum involution and lactation groups (n = 3 to 7 mice per group). In the postpartum involution group, the pups were fostered to the lactating mice immediately after delivery at 4 weeks post-chamber insertion, and their mammary glands allowed to involute for 3 weeks. Material from the biochambers was harvested at 4 weeks post-chamber insertion for the nulliparous and pregnant groups (within 24 hours of delivery of pups for pregnant group), and at 7 weeks for the postpartum involution and lactation groups, for histologic and radiographic examination.

Histologic and radiographic assessment of murine mammary fat pads (MFP's) during the various murine peripartum states

The MFP's of these nulliparous, pregnant, lactating and postpartum involution mice were also harvested for histologic (haematoxylin and eosin (H+E)) and radiographic assessment, to examine for associated changes related to the altered hormonal milieu during the various murine postpartum states.

Maintenance in biochambers of nulliparous mice for different durations

High and low MD tissues were maintained in separate biochambers in nulliparous mice then harvested at four, six and 12 weeks for histologic and radiographic examination, to determine if any changes in tissue composition or radiographic density were observed with different durations of biochamber maintenance.

Histological analysis and Immunohistochemistry (IHC)

Paraffin-embedded tissue sections (4 μm) of high and low MD biochamber tissues were stained with H+E, then assessed histologically with digital photomicroscopy. Images were imported into image analysis software JMicroVision v1.2.7 (Geneva, Switzerland) for threshold-masking to quantify the absolute areas and percent areas of stromal and glandular tissue components. The adipose area was calculated by subtracting stromal and glandular areas from the total area.

IHC staining with proliferation marker Ki67 (Clone MIB-1, Code M7240, DakoCytomation, Denmark) and antibody to human milk product, casein (Ab47972 Clone# F20.14, Abcam, Cambridge, UK), was performed to examine if there was a difference in proliferation with involution in high and low MD biochamber tissue, and if the xenograft human glandular structures were functional.

Radiographic analysis of biochamber tissues

As previously described, high and low MD biochamber tissues were examined with Faxitron imaging (Faxitron X-ray Corp., Arizona, USA, Model MX-20; 35 keV, 10 s). A calibration strip comprising exponentially stepped transparency sheets was used with each film [19]. Matched pairs of propagated high and low MD biochamber cores were cut to the same thickness (2 mm) before they were imaged. Image analysis

software (JMicroVision v1.2.7) was used to determine the mode of signal intensity for each core, compared to the signal intensity of the calibration strip.

Statistical analysis

Normality was assessed with D'Agostino and Pearson Omnibus normality test prior to determining statistical significance using GraphPad Prism 5.0 (California, USA). Where matched pairs of high and low biochamber tissues were compared within hormonal exposure groups, the data was treated as paired data. To compare the percentage tissue composition, glandular counts and relative densitometry of the high and low MD biochamber tissues harvested, paired t tests or unpaired t tests were used for parametric paired or unpaired data respectively. For non-parametric data, Wilcoxon rank sum tests or Mann Whitney tests were used to compare matched or unpaired data respectively (GraphPad Prism 5.0). The Kruskal-Wallis test was used to compare across more than two groups of non-parametric data. The p value of significance for rejecting a null hypothesis was 0.05.

Results

Study sample

The study sample consisted of high and low MD biopsies from within-individual breasts of ten high-risk women undergoing prophylactic mastectomy at St Vincent's Hospital Melbourne. The demographic characteristics of the study women are listed in Tables 1 and 2. The women were at increased risk of malignancy due to strong family history of BC, having a BRCA1/2 mutation or a past history of BC.

Descriptive histologic changes of biochamber tissue after murine postpartum mammary involution, lactation and during pregnancy

No difference was seen in the glandular morphology between high and low MD biochamber tissues from nulliparous mice, and there was a preponderance of small lobules observed in the high and low MD biochamber tissue harvested from the nulliparous mice, as seen previously in the biochamber model of human MD [19].

H+E sections of high and low MD biochamber tissues harvested from pregnant and lactation groups demonstrated enlarged lobules compared to glands in the MD tissues of the nulliparous group, with vacuolated epithelial cells and small amounts of secretion in distended lumens, and decreased stroma (Figs.1, 3b). With postpartum involution, the glandular area in both high and low MD biochamber tissues were also increased compared to nulliparous mice, with a mixture of large and small lobules. Luminal secretions and debris were visible in the glands of the biochamber tissues of the involution group (Fig. 1). There was an influx of inflammatory infiltrate into the biochambers, mainly macrophages, during murine pregnancy and involution, in keeping with established histologic observations of human breast tissue in pregnancy, lactation and involution [25].

Ki67, anti-casein and Oil Red-O staining

Ki67 nuclear staining occurred predominantly in glandular epithelium, and to a lesser extent in stromal and adipose cells (Fig 2). Increased Ki67 staining of the glandular component was seen in high compared to low MD biochamber tissues during murine pregnancy (Fig 2). However, there was no difference in Ki67 counts in high compared to low MD biochamber tissues during early postpartum involution (Fig 2).

Immunohistochemical staining with human anti-casein antibody demonstrated occasional milk proteins in the cytoplasm and lumen of glandular epithelium of biochamber tissue in pregnant and lactating mice (Fig 3a). Lipid-containing vacuoles within high and low MD biochamber tissues stained red with Oil Red-O, and secretions or debris were observed in the glandular lumen within the biochamber tissues during murine pregnancy and lactation (Fig. 3b).

Quantitative analysis of biochamber tissue

Analysis of tissue composition (percentage area) of high MD biochamber tissues harvested from postpartum involution compared to nulliparous mice demonstrated that high MD biochamber tissue from postpartum involution mice had decreased stromal percentage area ($p=0.0027$), increased adipose percentage area ($p=0.0003$) and a trend to increased glandular percentage area ($p=0.076$) (Fig. 4b). High MD biochamber tissues from lactating mice also had decreased stromal ($p=0.042$), increased adipose ($p=0.009$) and glandular percentage area ($p=0.001$) compared to nulliparous mice (Fig. 4c). However, there was no difference in stromal, adipose or glandular percentage area in high MD biochamber tissues harvested at 4 weeks between nulliparous and pregnant mice, or that harvested at 7 weeks, between lactating and involuting mice (Fig. 4a,d).

In the low MD biochamber tissues, no difference was observed in the stromal, adipose or glandular percentage area between nulliparous and pregnant mice, nulliparous and postpartum involution mice, or nulliparous and lactating mice (Fig 5).

No difference was observed in the gland counts between high MD biochamber tissues from nulliparous, pregnant, postpartum involution and lactating mice ($p=0.9168$); or between low MD biochamber tissues from these mice groups ($p=0.9320$) (Fig. 6a).

There was no difference in gland counts comparing high and low MD biochamber tissues in each of the nulliparous, pregnant or postpartum involution groups (Fig. 6b).

Radiographic changes of biochamber tissue after postpartum mammary involution

Analysis of x-ray signal intensity demonstrated increased x-ray relative densitometry of biochamber tissues during murine postpartum involution compared to pregnant and nulliparous mice, in both high ($p=0.0021$) and low MD biochamber tissues ($p=0.0004$) (Fig. 7a). Quantitative analysis of relative densitometry revealed a trend to decreased x-ray density in low compared to high MD biochamber tissues in nulliparous mice ($p=0.0534$) (Fig. 7b). There was no difference in x-ray density of high and low MD biochamber tissues in pregnant or postpartum involution mice (Fig. 7b).

Histologic and radiographic assessment of MFP's during the various murine peripartum states

H+E sections of MFP's during pregnancy demonstrated dilated ducts and lobules surrounded by fat, with the presence of protein in the lumen of the glands (Fig. 8b). During postpartum involution, the alveoli collapsed into clusters of epithelial cells, and stroma increased around the collapsed structures (Fig. 8c). During lactation, the alveoli in the MFP expanded to completely fill the gland, with flattened epithelial cells in the process of secreting milk fat droplets visible on H+E sections (Fig. 8d). These findings are similar to established histological changes observed in MFP's during various murine peripartum states [26]. The relative densitometry of the MFP's altered between the various peripartum states ($p=0.0332$) (Fig 9e).

Maintenance in biochambers of nulliparous mice for different durations

High and low MD tissues maintained in separate biochambers in nulliparous mice for 4, 6 and 12 weeks did not demonstrate any changes in stromal, adipose or glandular percentage area over the different durations (Figs. 9a, b). Radiographic examination of the high and low biochamber tissues at 4 and 12 weeks in nulliparous mice demonstrated increased radiographic density at 12 weeks ($p=0.005$, $p=0.006$) (Fig. 9c).

Discussion

MD, BC risk and response to systemic hormonal states

A transient increase in BC risk has been observed up to 5 years postpartum, before falling below the woman's baseline risk [27-29]. Each additional live birth may decrease BC risk by 9%, while 6 months of breast-feeding may decrease the risk by a further 5% [30]. During pregnancy and early postpartum involution, MD has also been observed to increase, but over a shorter time period. Subsequent to each live birth, the probability of having high MD decreased [31-33], suggesting that decreasing MD may mediate the protective effect of parity against BC [33]. It is unclear whether MD may affect the risk of pregnancy-associated BC (PABC) through biocellular interactions during early postpartum involution, or if the increased MD and its associated risk in early involution reflects the increased volume of fibroglandular tissue at risk. Postpartum BC development could also be caused by hormones of pregnancy that promote proliferation of pre-initiated target cell populations [34]. Oestrogen may increase PABC risk via increased systemic angiogenesis, stromalization and bone marrow cell recruitment, rather than classic proliferative effects of ER binding [34].

It is well-established that standard HRT such as estrogen and progesterone (E+P) and estrogen only (E) HRT can increase MD in post-menopausal women, and that cessation of HRT results in a reduction in MD [35,36,15]. Moreover, an association between E+P HRT use and high MD was observed in patients who later developed BC, suggesting that the response of breast tissue to exogenous hormones may lead to BC development via MD-related mechanisms. An important observation that Tamoxifen decreased MD and MD-associated cancer risk in BC survivors [18] suggests the possibility of future preventative strategies to monitor and reduce MD-associated risk through current mammographic screening programs, and pharmacological interventions to reduce MD.

Recent work has suggested that pro-oncogenic tissue-remodelling in extracellular matrix (ECM) during postpartum involution may play a role in promoting cancer [28,37]. ECM mediators implicated in mammary involution (e.g. fibronectin, MMP2 and MMP9) also affect MD [37,38]. In early postpartum involution, massive apoptosis of secretory epithelium occurs, the stromal compartment increases, while fibroblasts secrete proteases that degrade ECM proteins. This then attracts inflammatory infiltration by chemotaxis, including macrophages and neutrophils; all resulting in a pro-tumorigenic microenvironment that promotes invasiveness and tumour cell motility [39,28]. Further studies to examine the influence of pro-oncogenic ECM and immune cell function in mediating MD-associated cancer risk will be useful.

Morphologic changes in biochamber glandular structures and tissue microenvironment after lactation and postpartum involution

A decrease in stromal and increased gland areas was observed with lactation and postpartum involution at 7 weeks, however, the gland counts remained unchanged, suggesting that morphological changes occurred in response to the postpartum hormonal changes in this model, or due to the increased duration of MD tissue within the biochambers. Moreover, casein staining revealed occasional human milk protein products in the glandular epithelium of biochamber tissues, indicating that the human breast tissue may function partially in response to murine systemic hormones of pregnancy.

An influx of immune cells, including macrophages, into the biochamber was observed during pregnancy and postpartum involution. The increased numbers of macrophages are in keeping with known histologic findings in human breast tissue during pregnancy and involution, and further support the dynamic nature of the xenograft model where circulating immune cells are appropriately recruited into the MD tissues during different peripartum states [25,28].

Reduction in stromal area with increased adipose and gland area after postpartum involution or lactation in high MD tissue

Quantitative histological analysis revealed increased adipose and reduced stromal percent areas in high MD biochamber tissues after postpartum involution or lactation compared to nulliparous mice, and increased glandular area in lactating compared to nulliparous mice, suggesting that the histologic changes may be related to alteration in the murine hormonal milieu during involution and lactation, or due to the different duration of biochamber maintenance. However, our observation that there was no difference in the histologic composition of high and low MD biochamber tissues maintained in nulliparous mice at different time points (Figs. 9a, b) lends support to

the hypothesis that the dynamic changes in the biochamber system may be due to altered peripartum hormones rather than biochamber duration.

The increase in radiographic density in biochamber tissues in postpartum involution compared to nulliparous mice, together with the reduction in stromal percent areas in postpartum involution biochamber tissues, suggests that the increased MD could be related to ECM mechanoregulation in high MD tissues [40]. Alternatively, paracrine factors released during various peripartum states, such as TGF-β, which is responsible for apoptosis, and mammary gland remodelling during early postpartum involution may also play a role [41-43].

Increase in radiographic density in early postpartum involution in high and low MD biochamber tissues

We observed increased radiographic density in high and low MD biochamber tissues maintained in biochambers of postpartum involution mice for 7 weeks compared to the 4 week controls (Fig. 7a). Additional radiographic analyses of high or low MD tissues maintained in biochambers for 4 or 12 weeks demonstrated increased x-ray density with the longer biochamber duration (Fig. 9c). This suggests that increased radiographic density may occur in response to the systemic endocrine milieu in early postpartum mice, or over time.

The increased radiographic density observed in biochamber tissues after murine postpartum involution is in keeping with other observations that increased radiographic density is seen on mammograms of women in the early postpartum period [44]. Moreover, BC risk is increased in the postpartum period, with more aggressive tumours that metastasize [28]. Histological examination of the biochamber tissues during early involution suggest that the increased radiographic density may be

related to residual glandular secretions, increased glandular area or ECM deposition. We did not see any evidence of the increased dense connective tissue that we [20] and others [45] have associated with increased MD in women.

Morphological changes in murine MFP during different peripartum states

The changes in murine MFP observed with murine pregnancy, lactation and early postpartum involution (Figs. 8 a-c) demonstrate that the expected effects of systemic endocrine alterations associated with different peripartum states occurred in the host mice [26]. Moreover, these changes suggest that there are sufficiently high levels of endogenous hormones of pregnancy to model the changes that normally occur in MFPs and thus human MD tissue during these reproductive stages. These observed peripartum histologic changes in murine MFPs further support that the xenograft host environment is dynamic.

Strengths and limitations

The changes observed in the biochamber tissue composition and radiographic density with altered hormonal milieu during various murine peripartum states, or increased duration of biochamber maintenance, demonstrate the dynamic nature of the xenograft model. Thus, the xenograft tissue may be amenable to other interventions, including future drug interventions or investigation of individual cell subpopulations that may be responsible for MD-associated BC risk. This is the first study to demonstrate that functional human breast tissue of differing MD can be viably maintained in a murine model and can respond in a dynamic manner.

A limitation of this study is that the MD tissue was harvested at different time points due to logistical issues with the number of chambers that can be inoculated at one sitting: at 4 weeks after delivery of the pups for pregnancy and nulliparous groups, or after postpartum involution or lactation at 7 weeks. While histologic assessment of high and low MD biochamber tissue at three different time points did not demonstrate a difference in tissue composition, suggesting that biochamber tissue composition is not affected by duration of biochamber maintenance, differences in radiographic density was observed at different timepoints. Further experiments to examine differences between high and low MD biochamber tissues maintained in nulliparous compared to postpartum involution or lactating mice at 7 weeks may inform if the changes in MD are indeed due to hormonal influences rather than the duration of tissue maintenance in the biochamber system. It is likely that histologic changes observed with involution or lactation may occur mainly in the early postpartum period, and further changes may ensue over time to reflect decreased MD during late postpartum involution.

Future studies examining the effects of pharmacologic intervention with MD-modifying drugs such as Tamoxifen upon MD breast tissue histology, radiographic density and cell proliferation will also be useful, given the correlation with BC risk reduction [18].

Conclusion

Radiographic density in high and low MD biochamber human breast tissue increased after maintenance in biochambers during early postpartum murine mammary involution. Quantitative analysis of high MD biochamber tissue sections revealed decreased stromal, increased adipose and glandular area in postpartum involution

compared to nulliparous mice, and in lactating compared to nulliparous mice. These findings are significant as they demonstrate the dynamic nature of the MD xenograft model, where the changes may occur due to alterations in the murine hormonal milieu, or differences in duration of biochamber propagation. The biochamber system may be amenable to future pharmacological intervention and genetic analysis of candidates in a preclinical model.

Competing interests

The authors declare that they have no competing interests.

Acknowledgements

This work was supported by the Victorian BC Research Consortium (MCS, EWT, JH), the St Vincent's Hospital Research Endowment Fund (EWT 2008, 2009), and National Health and Medical Research Council (GLC, MCS, JH) and the University of Melbourne Research Grant Support Scheme (MRGSS; EWT, IH, GLC). We thank Sue MacAuley and Nadine Wood (St Vincent's BreastScreen, St Vincent's Hospital, Victoria) for help with radiography and tissue sampling. St Vincent's Institute receives support from the Victorian Government's Operational Infrastructure Support Program.

Figure Legends

Fig. 1 H+E staining of high and low MD biochamber tissues harvested from nulliparous mice, mice immediately post-parturition (pregnancy group), during early postpartum involution and lactation demonstrate the morphological changes in glandular and stromal tissues.

Fig. 2 Ki67 staining of high and low MD biochamber tissues harvested from mice immediately post-parturition (pregnancy group), during early postpartum involution and lactation demonstrate increased nuclear staining in high compared to low MD

biochamber tissue during lactation and pregnancy qualitatively, but no difference in Ki67 counts during postpartum involution.

Fig. 3 Anti-casein staining of MD biochamber tissues harvested from mice immediately post-parturition (pregnancy group), during early postpartum involution and lactation demonstrate infrequent cytoplasmic and staining of the milk protein during murine pregnancy, involution and lactation.

Fig. 4 a) The scatter plot column graph comparing high MD biochamber tissues harvested from nulliparous and mice immediately post-parturition (pregnancy group) did not reveal a difference between stromal, adipose or glandular areas; b) The scatter plot column graph comparing high MD biochamber tissues harvested from nulliparous and postpartum involution mice demonstrated decreased stromal, increased adipose and increased glandular areas in the postpartum involution group; c) The scatter plot column graph comparing high MD biochamber tissues harvested from nulliparous and lactating mice demonstrated decreased stromal, increased adipose and increased glandular areas in the lactating group; d) The scatter plot column graph comparing high MD biochamber tissues harvested from postpartum involution and lactating mice did not reveal a difference between stromal, adipose or glandular areas.

Fig. 5 a) The scatter plot column graph comparing low MD biochamber tissues harvested from nulliparous and mice immediately post-parturition (pregnancy group) did not reveal a difference between stromal, adipose or glandular areas; b) The scatter plot column graph comparing low MD biochamber tissues harvested from nulliparous and postpartum involution mice did not reveal a difference between stromal, adipose or glandular areas; c) The scatter plot column graph comparing low MD biochamber

tissues harvested from nulliparous and lactating mice did not reveal a difference between stromal, adipose or glandular areas; d) The scatter plot column graph comparing high MD biochamber tissues harvested from postpartum involution and lactating mice did not reveal a difference between stromal, adipose or glandular areas.

Fig. 6 a) The scatter plot column graph comparing the glandular counts of high and low MD biochamber tissues harvested from nulliparous and mice immediately post-parturition (pregnancy group) did not reveal a difference. There was also no difference between the glandular counts of high and low MD biochamber tissues harvested from postpartum involution and lactating mice; b) The scatter plot column graph comparing the glandular counts of high and low MD biochamber tissues harvested from nulliparous mice did not demonstrate a difference. Likewise, there was no difference in the glandular counts of high and low MD biochamber tissues harvested from the pregnancy, postpartum involution or lactating groups.

Fig. 7 a) The scatter plot column graph comparing the x-ray densitometry of high MD biochamber tissues harvested from nulliparous, pregnant and postpartum involution mice revealed a significant increase in relative densitometry units with postpartum involution. The scatter plot column graph comparing the x-ray densitometry of low MD biochamber tissues harvested from nulliparous, pregnant and postpartum involution mice revealed a significant increase in relative densitometry units with postpartum involution; b) The scatter plot column graph comparing the x-ray densitometry of high and low MD biochamber tissues harvested from nulliparous mice demonstrated a trend towards decreased relative densitometry units in low MD tissues, but no difference in x-ray densitometry of high and low MD biochamber tissues in the pregnant or postpartum involution groups.

Fig. 8 a) H+E section of a MFP of a nulliparous mouse with branching glands in adipose tissue. b) The H+E section of a MFP during pregnancy demonstrated dilated ducts and lobules surrounded by fat, with the presence of protein, stained pink/purple (indicated by a yellow arrow), in the lumen of the glands. c) The H+E section of a MFP during postpartum involution demonstrated a few apoptotic bodies (yellow arrow). The alveoli in the MFPs have collapsed into clusters of epithelial cells (yellow asterisk), and stroma had increased around the collapsed structures. d) The H+E section of a MFP during lactation demonstrated alveoli that have expanded to completely fill the gland, with flattened epithelial cells in the process of secreting milk fat droplets easily visible at high-powered magnification (yellow arrow). d) The scatter plot column graph comparing the x-ray densitometry of MFP's harvested from parous, lactating and postpartum involution mice demonstrate alterations in relative densitometry.

Fig. 9 a) The scatter plot column graph comparing the percentage tissue area of high MD biochamber tissues harvested from nulliparous mice at 4, 6 and 12 weeks did not demonstrate a difference. b) The scatter plot column graph comparing the percentage tissue area of low MD biochamber tissues harvested from nulliparous mice at 4, 6 and 12 weeks did not demonstrate a difference. c) The scatter plot column graph comparing the x-ray densitometry of high and low MD biochamber tissues harvested from nulliparous mice at 4, 6 and 12 weeks did not demonstrate a difference in radiographic density.

Supplementary Figure Legend

Supp Fig. 1 a) The scatter plot column graph comparing the percentage tissue area of high MD biochamber tissues harvested from pregnant and lactating mice did not

demonstrate a difference between stromal and fat percentage areas. An increase in gland percentage area was observed in high MD biochamber tissues harvested from lactating compared to pregnant mice. b) The scatter plot column graph comparing the percentage tissue area of high MD biochamber tissues harvested from pregnant and postpartum involution mice did not demonstrate a difference.

Tables

Table 1 Demographic characteristics of participants in the study, including their age, Birads score, family history, menopausal status, parity and past history of breast disease.

Demographic characteristics	Number, N, or Mean
Age	Mean 45.6 years (Range 38 – 57 years)
Birads category 4 3 2 1	 2 4 4 0
Family history Nil BRCA-, strong FHx BRCA2+	 4 3 3
Menopausal status Pre Peri	 9 1

Post	0
Past history of breast disease Yes – BC or DCIS No	 6 4
Parity Parous Nulliparous	 7 3

Birads score 1: Predominantly fat, 2: Scattered fibroglandular densities, 3: Heterogeneously dense, 4: Extremely dense. BC = BC. FHx = Family history. IDC = invasive ductal carcinoma. DCIS = ductal carcinoma in situ.

Table 2 Histopathology results of operative specimens from study cohort, including operation performed and histology findings.

Participant	Operation performed	Histology findings
1	Left skin sparing mastectomy - sample was from left side	Left mastectomy: 6 mm DCIS with microcalcification, FCC
2	Left skin sparing mastectomy - sample was from	Left mastectomy: FCC with fibrosis and adenosis

	left side	
3	Right skin sparing mastectomy - sample was from right side	Right mastectomy: FCC, apocrine metaplasia
4	Left skin sparing mastectomy - sample was from left side	Left mastectomy: 65 mm DCIS with comedo necrosis, FCC, apocrine metaplasia
5	Bilateral skin sparing mastectomy - sample was from left side	Left and right mastectomy: FCC
6	Left skin sparing mastectomy - sample was from left side	Left mastectomy: FCC
7	Bilateral skin sparing mastectomy - sample was from	Left mastectomy: 8 mm IDC, adjacent DCIS, ER 90%, PR 90%, Her2 negative. SN negative.

	left side	
8	Right skin sparing mastectomy - sample was from right side	Right mastectomy: 35 mm DCIS, 3 mm IDC, ER>90%, PR 1%, Her2 negative. SN negative
9	Bilateral skin sparing mastectomy - sample was from left side	Left and right mastectomy: ALH, sclerosing adenosis
10	Left skin sparing mastectomy - sample was from left side	Left mastectomy: 20 mm DCIS with necrosis and microcalcification

DCIS = ductal carcinoma in situ. IDC = invasive ductal carcinoma. FCC = fibrocystic change. MDE = mammary duct ectasia. ALH = atypical lobular hyperplasia. ER = oestrogen receptor, PR = progesterone receptor.

References

1. Boyd NF, Guo H, Martin LJ, Sun L, Stone J, Fishell E, Jong RA, Hislop G, Chiarelli A, Minkin S, Yaffe MJ (2007) Mammographic density and the risk and detection of breast cancer. N Engl J Med 356 (3):227-236. doi:356/3/227 [pii]
10.1056/NEJMoa062790

2. McCormack VA, dos Santos Silva I (2006) Breast density and parenchymal patterns as markers of breast cancer risk: a meta-analysis. Cancer Epidemiol Biomarkers Prev 15 (6):1159-1169. doi:15/6/1159 [pii]
10.1158/1055-9965.EPI-06-0034

3. Ursin G, Ma H, Wu AH, Bernstein L, Salane M, Parisky YR, Astrahan M, Siozon CC, Pike MC (2003) Mammographic density and breast cancer in three ethnic groups. Cancer Epidemiol Biomarkers Prev 12 (4):332-338

4. Byrne C, Schairer C, Wolfe J, Parekh N, Salane M, Brinton LA, Hoover R, Haile R (1995) Mammographic features and breast cancer risk: effects with time, age, and menopause status. J Natl Cancer Inst 87 (21):1622-1629

5. Boyd NF, Byng JW, Jong RA, Fishell EK, Little LE, Miller AB, Lockwood GA, Tritchler DL, Yaffe MJ (1995) Quantitative classification of mammographic densities and breast cancer risk: results from the Canadian National Breast Screening Study. J Natl Cancer Inst 87 (9):670-675

6. Wolfe JN, Saftlas AF, Salane M (1987) Mammographic parenchymal patterns and quantitative evaluation of mammographic densities: a case-control study. AJR Am J Roentgenol 148 (6):1087-1092

7. Byrne C, Schairer C, Brinton LA, Wolfe J, Parekh N, Salane M, Carter C, Hoover R (2001) Effects of mammographic density and benign breast disease on breast cancer risk (United States). Cancer Causes Control 12 (2):103-110

8. MacMahon B, Cole P, Lin TM, Lowe CR, Mirra AP, Ravnihar B, Salber EJ, Valaoras VG, Yuasa S (1970) Age at first birth and breast cancer risk. Bull World Health Organ 43 (2):209-221

9. Franceschi S (1989) Reproductive factors and cancers of the breast, ovary and endometrium. Eur J Cancer Clin Oncol 25 (12):1933-1943

10. Brinton LA, Schairer C, Hoover RN, Fraumeni JF, Jr. (1988) Menstrual factors and risk of breast cancer. Cancer Invest 6 (3):245-254

11. Britt K, Short R The plight of nuns: hazards of nulliparity. Lancet 379 (9834):2322-2323. doi:S0140-6736(11)61746-7 [pii]
10.1016/S0140-6736(11)61746-7

12. Purdie DM, Bain CJ, Siskind V, Webb PM, Green AC (2003) Ovulation and risk of epithelial ovarian cancer. Int J Cancer 104 (2):228-232. doi:10.1002/ijc.10927

13. Li T, Sun L, Miller N, Nicklee T, Woo J, Hulse-Smith L, Tsao MS, Khokha R, Martin L, Boyd N (2005) The association of measured breast tissue characteristics with mammographic density and other risk factors for breast cancer. Cancer Epidemiol Biomarkers Prev 14 (2):343-349. doi:14/2/343 [pii]
10.1158/1055-9965.EPI-04-0490

14. Martin LJ, Minkin S, Boyd NF (2009) Hormone therapy, mammographic density, and breast cancer risk. Maturitas 64 (1):20-26. doi:S0378-5122(09)00231-X [pii]
10.1016/j.maturitas.2009.07.009

15. Greendale GA, Reboussin BA, Slone S, Wasilauskas C, Pike MC, Ursin G (2003) Postmenopausal hormone therapy and change in mammographic density. J Natl Cancer Inst 95 (1):30-37

16. Lundstrom E, Christow A, Kersemaekers W, Svane G, Azavedo E, Soderqvist G, Mol-Arts M, Barkfeldt J, von Schoultz B (2002) Effects of tibolone and continuous combined hormone replacement therapy on mammographic breast density. Am J Obstet Gynecol 186 (4):717-722. doi:S0002937802284860 [pii]

17. Rutter CM, Mandelson MT, Laya MB, Seger DJ, Taplin S (2001) Changes in breast density associated with initiation, discontinuation, and continuing use of hormone replacement therapy. JAMA 285 (2):171-176. doi:joc01079 [pii]

18. Cuzick J, Warwick J, Pinney E, Duffy SW, Cawthorn S, Howell A, Forbes JF, Warren RM (2011) Tamoxifen-induced reduction in mammographic density and breast cancer risk reduction: a nested case-control study. J Natl Cancer Inst 103 (9):744-752. doi:djr079 [pii] 10.1093/jnci/djr079

19. Chew GL, Huang D, Lin SJ, Huo C, Blick T, Henderson MA, Hill P, Cawson J, Morrison WA, Campbell IG, Hopper JL, Southey MC, Haviv I, Thompson EW (2012) High and low mammographic density human breast tissues maintain histological differential in murine tissue engineering chambers. Breast Cancer Res Treat 135 (1):177-187. doi:10.1007/s10549-012-2128-z

20. Lin SJ, Cawson J, Hill P, Haviv I, Jenkins M, Hopper JL, Southey MC, Campbell IG, Thompson EW (2011) Image-guided sampling reveals increased stroma and lower glandular complexity in mammographically dense breast tissue. Breast Cancer Res Treat 128 (2):505-516. doi:10.1007/s10549-011-1346-0

21. Boyd NF, Melnichouk O, Martin LJ, Hislop G, Chiarelli AM, Yaffe MJ, Minkin S (2011) Mammographic density, response to hormones, and breast cancer risk. J Clin Oncol 29 (22):2985-2992. doi:JCO.2010.33.7964 [pii] 10.1200/JCO.2010.33.7964

22. Kelly JL, Findlay MW, Knight KR, Penington A, Thompson EW, Messina A, Morrison WA (2006) Contact with existing adipose tissue is inductive for adipogenesis in matrigel. Tissue Eng 12 (7):2041-2047. doi:10.1089/ten.2006.12.2041

23. Stillaert F, Findlay M, Palmer J, Idrizi R, Cheang S, Messina A, Abberton K, Morrison W, Thompson EW (2007) Host rather than graft origin of Matrigel-induced adipose tissue in the murine tissue-engineering chamber. Tissue Eng 13 (9):2291-2300. doi:10.1089/ten.2006.0382

24. Thomas GP, Hemmrich K, Abberton KM, McCombe D, Penington AJ, Thompson EW, Morrison WA (2008) Zymosan-induced inflammation stimulates neo-adipogenesis. Int J Obes (Lond) 32 (2):239-248. doi:0803702 [pii]
10.1038/sj.ijo.0803702

25. Rosen PP (ed) (2009) Rosen's Breast Pathology. 3rd Edition edn. Lippincott Williams & Wilkins, Philadelphia

26. Richert MM, Schwertfeger KL, Ryder JW, Anderson SM (2000) An atlas of mouse mammary gland development. J Mammary Gland Biol Neoplasia 5 (2):227-241

27. Albrektsen G, Heuch I, Hansen S, Kvale G (2005) Breast cancer risk by age at birth, time since birth and time intervals between births: exploring interaction effects. Br J Cancer 92 (1):167-175. doi:6602302 [pii]
10.1038/sj.bjc.6602302

28. Schedin P (2006) Pregnancy-associated breast cancer and metastasis. Nat Rev Cancer 6 (4):281-291. doi:nrc1839 [pii]
10.1038/nrc1839

29. Wohlfahrt J, Melbye M (2001) Age at any birth is associated with breast cancer risk. Epidemiology 12 (1):68-73

30. Milne RL, John EM, Knight JA, Dite GS, Southey MC, Giles GG, Apicella C, West DW, Andrulis IL, Whittemore AS, Hopper JL (2011) The potential value of sibling controls

compared with population controls for association studies of lifestyle-related risk factors: an example from the Breast Cancer Family Registry. Int J Epidemiol 40 (5):1342-1354. doi:dyr110 [pii]
10.1093/ije/dyr110
31. Lope V, Perez-Gomez B, Sanchez-Contador C, Santamarina MC, Moreo P, Vidal C, Laso MS, Ederra M, Pedraz-Pingarron C, Gonzalez-Roman I, Garcia-Lopez M, Salas-Trejo D, Peris M, Moreno MP, Vazquez-Carrete JA, Collado F, Aragones N, Pollan M (2012) Obstetric history and mammographic density: a population-based cross-sectional study in Spain (DDM-Spain). Breast Cancer Res Treat. doi:10.1007/s10549-011-1936-x
32. Loehberg CR, Heusinger K, Jud SM, Haeberle L, Hein A, Rauh C, Bani MR, Lux MP, Schrauder MG, Bayer CM, Helbig C, Grolik R, Adamietz B, Schulz-Wendtland R, Beckmann MW, Fasching PA (2010) Assessment of mammographic density before and after first full-term pregnancy. Eur J Cancer Prev 19 (6):405-412. doi:10.1097/CEJ.0b013e32833ca1f4
33. Sung J, Song YM, Stone J, Lee K, Lee D (2011) Reproductive factors associated with mammographic density: a Korean co-twin control study. Breast Cancer Res Treat 128 (2):567-572. doi:10.1007/s10549-011-1469-3
34. Gupta PB, Proia D, Cingoz O, Weremowicz J, Naber SP, Weinberg RA, Kuperwasser C (2007) Systemic stromal effects of estrogen promote the growth of estrogen receptor-negative cancers. Cancer Res 67 (5):2062-2071. doi:67/5/2062 [pii]
10.1158/0008-5472.CAN-06-3895
35. Couto E, Qureshi SA, Hofvind S, Hilsen M, Aase H, Skaane P, Vatten L, Ursin G Hormone therapy use and mammographic density in postmenopausal Norwegian women. Breast Cancer Res Treat 132 (1):297-305. doi:10.1007/s10549-011-1810-x
36. van Duijnhoven FJ, Peeters PH, Warren RM, Bingham SA, van Noord PA, Monninkhof EM, Grobbee DE, van Gils CH (2007) Postmenopausal hormone therapy and changes in mammographic density. J Clin Oncol 25 (11):1323-1328. doi:JCO.2005.04.7332 [pii]

10.1200/JCO.2005.04.7332

37. Bemis LT, Schedin P (2000) Reproductive state of rat mammary gland stroma modulates human breast cancer cell migration and invasion. Cancer Res 60 (13):3414-3418

38. Schenk S, Hintermann E, Bilban M, Koshikawa N, Hojilla C, Khokha R, Quaranta V (2003) Binding to EGF receptor of a laminin-5 EGF-like fragment liberated during MMP-dependent mammary gland involution. J Cell Biol 161 (1):197-209. doi:10.1083/jcb.200208145 jcb.200208145 [pii]

39. Lyons TR, O'Brien J, Borges VF, Conklin MW, Keely PJ, Eliceiri KW, Marusyk A, Tan AC, Schedin P (2011) Postpartum mammary gland involution drives progression of ductal carcinoma in situ through collagen and COX-2. Nat Med 17 (9):1109-1115. doi:nm.2416 [pii] 10.1038/nm.2416

40. Schedin P, Keely PJ (2011) Mammary gland ECM remodeling, stiffness, and mechanosignaling in normal development and tumor progression. Cold Spring Harb Perspect Biol 3 (1):a003228. doi:cshperspect.a003228 [pii] 10.1101/cshperspect.a003228

41. Strange R, Li F, Saurer S, Burkhardt A, Friis RR (1992) Apoptotic cell death and tissue remodelling during mouse mammary gland involution. Development 115 (1):49-58

42. Streuli CH, Schmidhauser C, Kobrin M, Bissell MJ, Derynck R (1993) Extracellular matrix regulates expression of the TGF-beta 1 gene. J Cell Biol 120 (1):253-260

43. Nguyen AV, Pollard JW (2000) Transforming growth factor beta3 induces cell death during the first stage of mammary gland involution. Development 127 (14):3107-3118

44. Sabate JM, Clotet M, Torrubia S, Gomez A, Guerrero R, de las Heras P, Lerma E (2007) Radiologic evaluation of breast disorders related to pregnancy and lactation. Radiographics 27 Suppl 1:S101-124. doi:27/suppl_1/S101 [pii] 10.1148/rg.27si075505

45. Ghosh K, Brandt KR, Reynolds C, Scott CG, Pankratz VS, Riehle DL, Lingle WL, Odogwu T, Radisky DC, Visscher DW, Ingle JN, Hartmann LC, Vachon CM (2012) Tissue composition of mammographically dense and non-dense breast tissue. Breast Cancer Res Treat 131 (1):267-275. doi:10.1007/s10549-011-1727-4

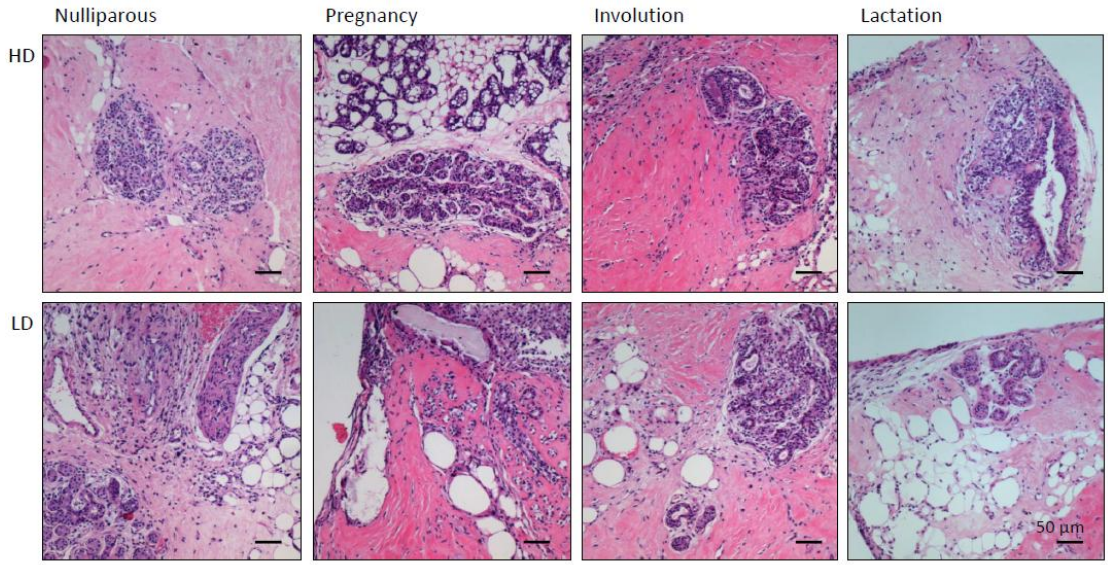

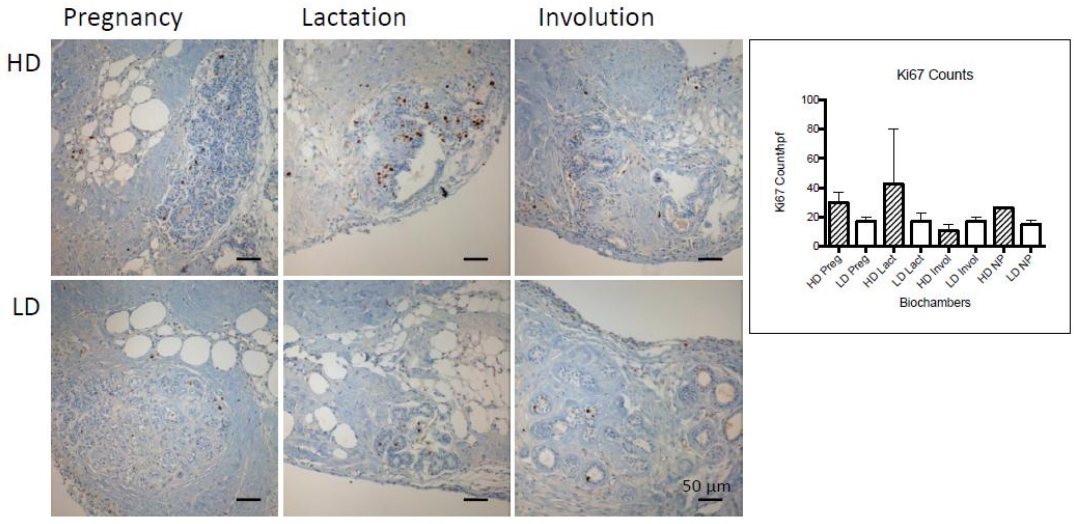

Fig. 3

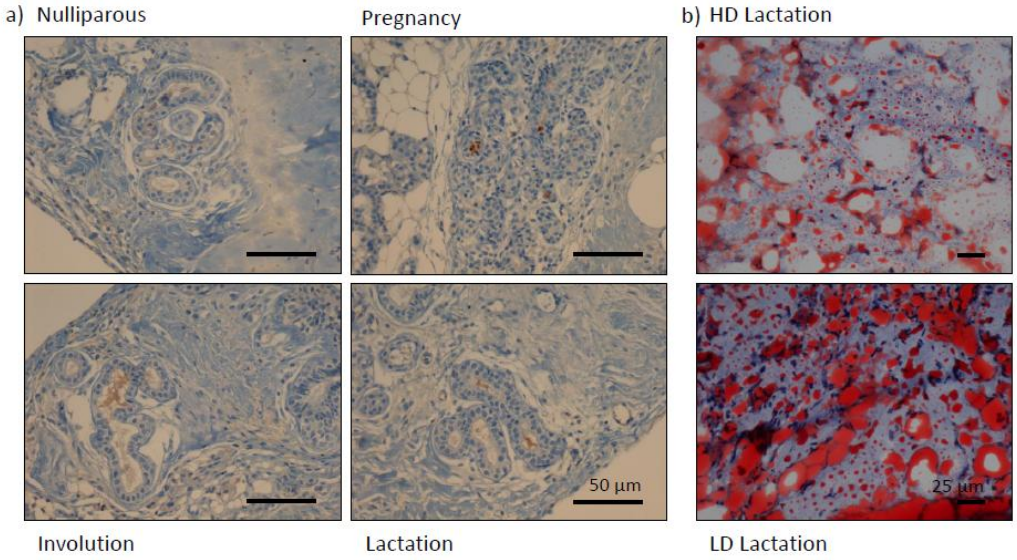
a) Nulliparous
Pregnancy
b) HD Lactation
50 µm
25 µm
Involution
Lactation
LD Lactation

Fig. 4

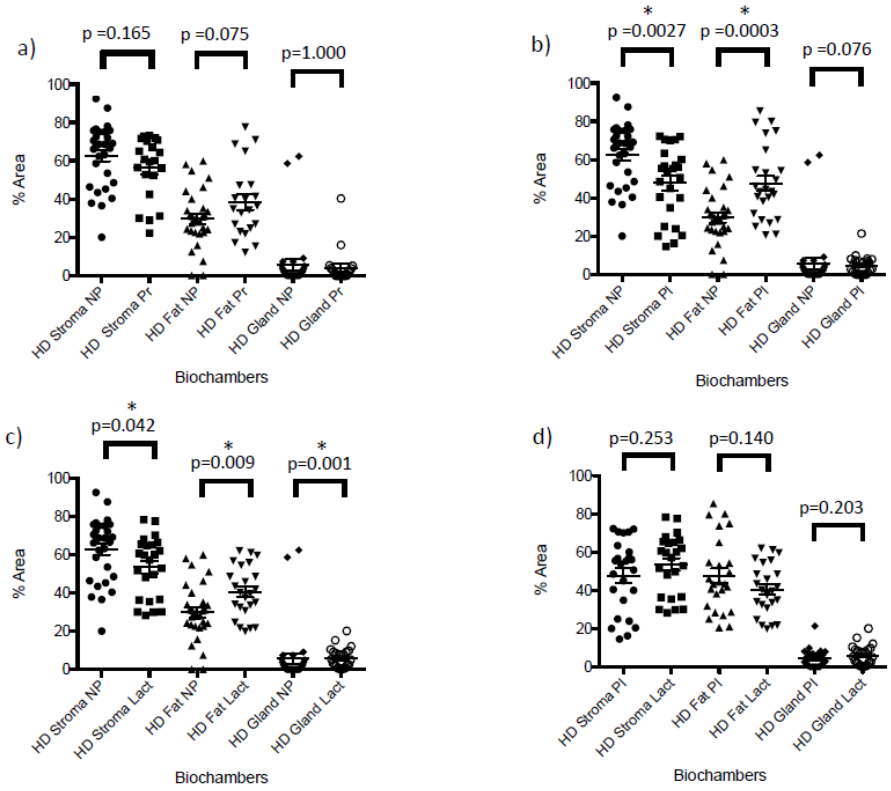
a)
p =0.165
p =0.075
p=1.000
% Area
HD Stroma NP
HD Stroma Pr
HD Fat NP
HD Fat Pr
HD Gland NP
HD Gland Pr
Biochambers
b)
*
p =0.0027
*
p =0.0003
p =0.076
HD Stroma PI
HD Fat PI
HD Gland PI
c)
*
p=0.042
*
p=0.009
*
p=0.001
HD Stroma Lact
HD Fat Lact
HD Gland Lact
d)
p=0.253
p=0.140
p=0.203

Fig. 5

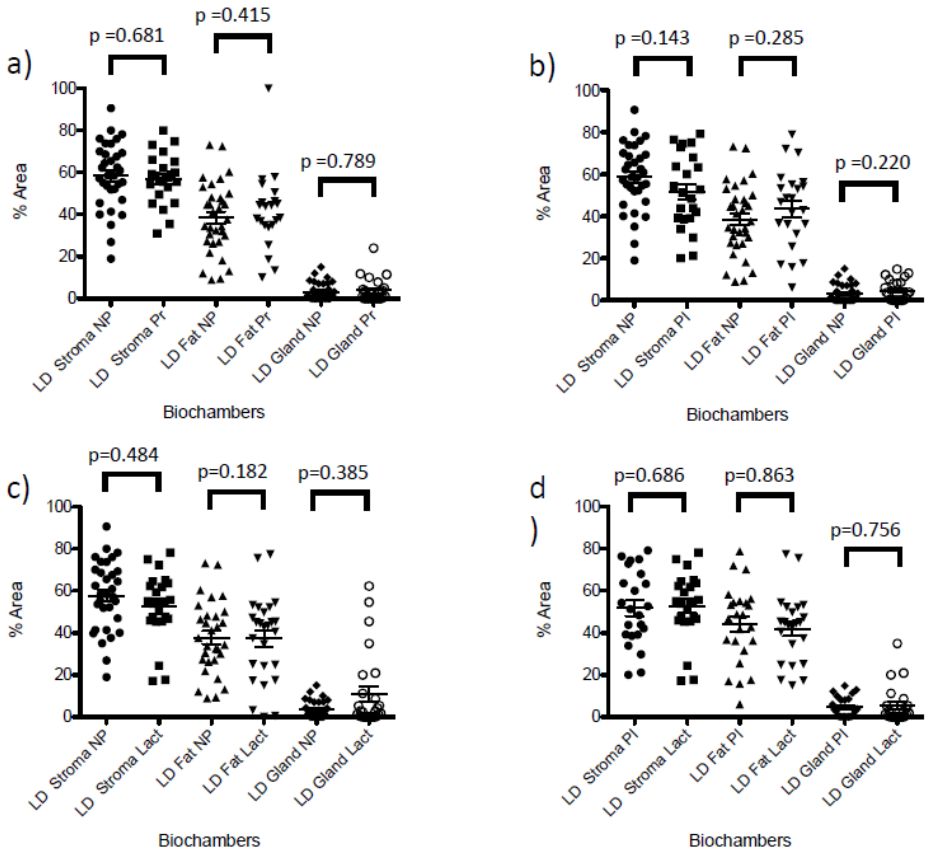
a)
p =0.681
p =0.415
p =0.789
% Area
LD Stroma NP
LD Stroma Pr
LD Fat NP
LD Fat Pr
LD Gland NP
LD Gland Pr
Biochambers
b)
p =0.143
p =0.285
p =0.220
% Area
LD Stroma NP
LD Stroma PI
LD Fat NP
LD Fat PI
LD Gland NP
LD Gland PI
Biochambers
c)
p=0.484
p=0.182
p=0.385
% Area
LD Stroma NP
LD Stroma Lact
LD Fat NP
LD Fat Lact
LD Gland NP
LD Gland Lact
Biochambers
d)
p=0.686
p=0.863
p=0.756
% Area
LD Stroma PI
LD Stroma Lact
LD Fat PI
LD Fat Lact
LD Gland PI
LD Gland Lact
Biochambers

Fig. 6

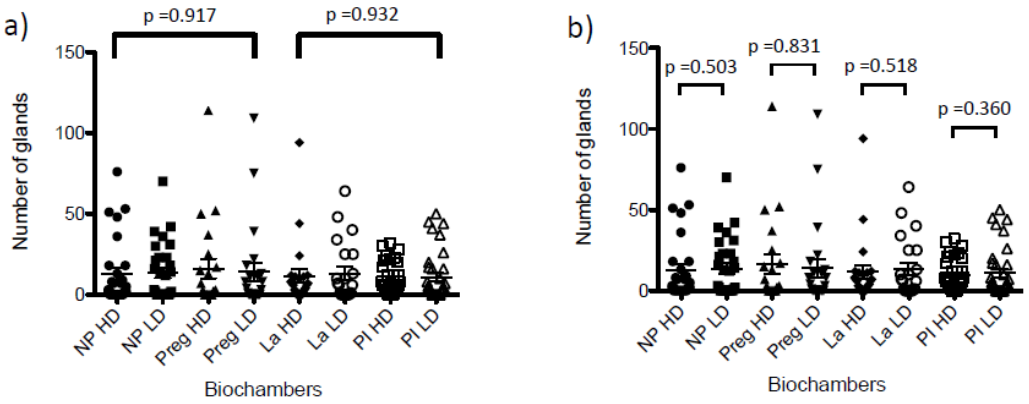
a)
p =0.917
p =0.932
Number of glands
150
100
50
0
NP HD
NP LD
Preg HD
Preg LD
La HD
La LD
PI HD
PI LD
Biochambers
b)
p =0.503
p =0.831
p =0.518
p =0.360
Number of glands
150
100
50
0
NP HD
NP LD
Preg HD
Preg LD
La HD
La LD
PI HD
PI LD
Biochambers

Fig. 7

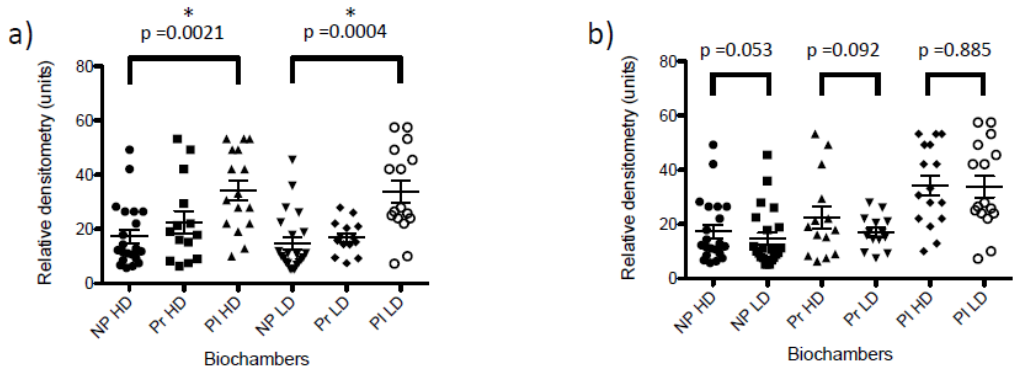
a)
*
p =0.0021
*
p =0.0004
Relative densitometry (units)
80
60
40
20
0
NP HD
Pr HD
PI HD
NP LD
Pr LD
PI LD
Biochambers
b)
p =0.053
p =0.092
p =0.885
Relative densitometry (units)
80
60
40
20
0
NP HD
NP LD
Pr HD
Pr LD
PI HD
PI LD
Biochambers

Fig. 8

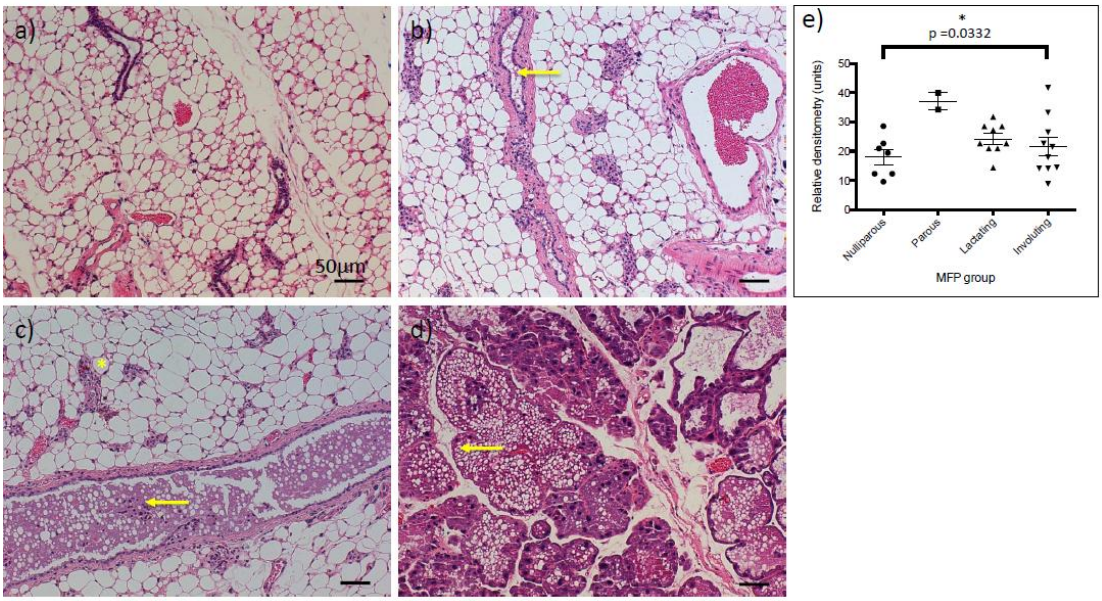
a)
50µm
b)
c)
d)
e)
*
p =0.0332
Relative densitometry (units)
50
40
30
20
10
0
Nulliparous
Parous
Lactating
Involuting
MFP group

Fig. 9

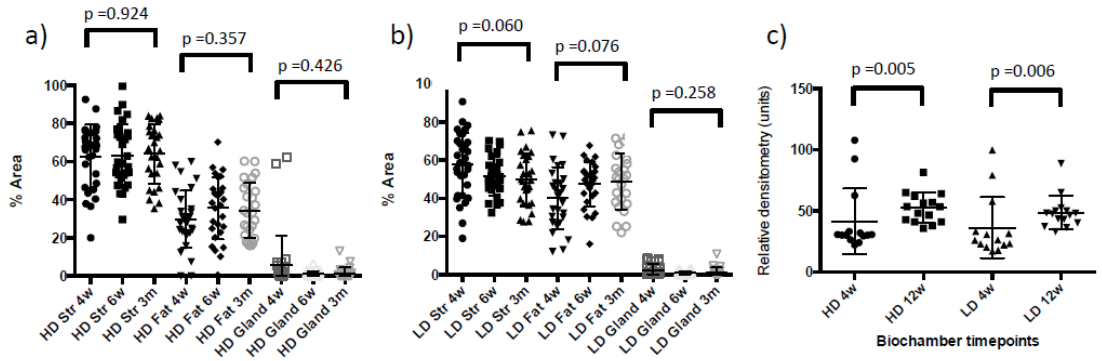
a)
p =0.924
p =0.357
p =0.426
% Area
100
80
60
40
20
0
HD Str 4w
HD Str 6w
HD Str 3m
HD Fat 4w
HD Fat 6w
HD Fat 3m
HD Gland 4w
HD Gland 6w
HD Gland 3m
b)
p =0.060
p =0.076
p =0.258
% Area
10
80
60
40
20
0
LD Str 4w
LD Str 6w
LD Str 3m
LD Fat 4w
LD Fat 6w
LD Fat 3m
LD Gland 4w
LD Gland 6w
LD Gland 3m
c)
p =0.005
p =0.006
Relative densitometry (units)
150
100
50
0
HD 4w
HD 12w
LD 4w
LD 12w
Biochamber timepoints

Author/s:
Chew, GL; Huang, D; Huo, CW; Blick, T; Hill, P; Cawson, J; Frazer, H; Southey, MD; Hopper, JL; Henderson, MA; Haviv, I; Thompson, EW

Title:
Dynamic changes in high and low mammographic density human breast tissues maintained in murine tissue engineering chambers during various murine peripartum states and over time

Date:
2013-07-01

Citation:
Chew, G. L., Huang, D., Huo, C. W., Blick, T., Hill, P., Cawson, J., Frazer, H., Southey, M. D., Hopper, J. L., Henderson, M. A., Haviv, I. & Thompson, E. W. (2013). Dynamic changes in high and low mammographic density human breast tissues maintained in murine tissue engineering chambers during various murine peripartum states and over time. BREAST CANCER RESEARCH AND TREATMENT, 140 (2), pp.285-297. https://doi.org/10.1007/s10549-013-2642-7.